Applied *Nanomaterials and smart Polymers,*
Online ISSN: 2981-0434
Vol. 2, No. 5

Role of Polymer Stabilization in Governing Oxytetracycline Adsorption on Graphene Oxide

Farand Farzi[1], Karim Zare[2], Omid Moradi[2]*, Kambiz Larijani[1]

[1]Department of Chemistry, SR.C, Islamic Azad University, Tehran, Iran.
[2]Department of Chemistry, ShQ.C, Islamic Azad University, Tehran, Iran.

***Corresponding Author:** o.moradi@qodsiau.ac.ir

https://doi.org/10.82428/ansp.2025.1224373

ABSTRACT

Oxytetracycline (OTC) is a widely used antibiotic that can persist in aquatic environments and raise environmental concerns. In this work, a graphene oxide/methyl methacrylate (GO/MMA) nanocomposite was synthesized via radical polymerization to explore how polymer stabilization influences the adsorption behavior of OTC on graphene oxide. The presence of the polymer matrix contributed to improved structural stability of GO and affected its interaction with OTC molecules.Adsorption experiments were carried out under optimized conditions, including pH 7.5, an adsorbent dosage of 0.3 g per 100 mL, an initial OTC concentration of 40 mg L^{-1}, a contact time of 90 min, and a temperature of 25 °C. Kinetic analysis showed that the adsorption followed a pseudo-second-order model (R^2 = 0.995), while equilibrium data were best described by the Langmuir isotherm, yielding a maximum adsorption capacity of 96 mg g^{-1} and indicating monolayer adsorption.Thermodynamic evaluation revealed that the adsorption process was spontaneous ($\Delta G°$ = –3.8 to –5.1 kJ mol^{-1}) and endothermic ($\Delta H°$ = +18.7 kJ mol^{-1}), accompanied by a positive entropy change ($\Delta S°$ = +52.3 J mol^{-1} K^{-1}). The adsorption mechanism involved π–π interactions, hydrogen bonding, and electrostatic attractions between OTC and the polymer-stabilized GO surface. In addition, the GO/MMA nanocomposite retained approximately 85% of its initial adsorption capacity after five reuse cycles, demonstrating the beneficial role of polymer stabilization in developing stable, metal-free graphene based adsorbents for antibiotic removal from water.

.**KEYWORDS*:*** Graphene oxide; Polymer stabilization; Oxytetracycline; Adsorption behavior; Metal-free adsorbent.

INTRODUCTION

Pharmaceutical contamination of aquatic systems has emerged as a global concern due to the extensive use and poor degradation of antibiotics. Among the most frequently detected and environmentally persistent pharmaceutical residues is oxytetracycline (OTC), a broad spectrum antibiotic widely administered for its bacteriostatic properties[1]. OTC is known to interfere with bacterial protein synthesis by binding to the 30S ribosomal subunit, but its incomplete metabolism and poor biodegradability lead to its accumulation in natural water bodies[2]. This accumulation not only disturbs aquatic microbial ecosystems but also contributes significantly to the emergence and spread of antibiotic resistance genes (ARGs), a phenomenon now recognized as one of the most pressing global health threats [3].

Given the challenges posed by pharmaceutical pollutants, adsorption-based techniques have gained increasing attention as promising alternatives, offering advantages such as low energy consumption, ease of operation, and the potential for adsorbent regeneration and reuse [4].

Graphene oxide (GO), a two-dimensional carbon-based nanomaterial rich in oxygen-containing functional groups (e.g., hydroxyl, epoxy, and carboxyl), has gained significant traction in environmental remediation research [5]. Its large specific surface area, hydrophilicity, and strong interactions with aromatic and polar molecules make it particularly effective in capturing a variety of contaminants through π–π stacking, hydrogen bonding, and electrostatic attraction [6]. However, pristine GO often suffers from limitations in structural integrity, reusability, and mechanical robustness under practical environmental conditions [7].

To address these shortcomings, researchers have explored the integration of GO with various polymers to create stable, hybrid adsorbents. Among these, methyl methacrylate (MMA), a monomer that forms poly(methyl methacrylate) (PMMA) upon polymerization, has shown notable promise[8]. MMA provides desirable physicochemical characteristics, including thermal stability, transparency, and mechanical strength[9]. When combined with GO, it not only enhances the durability of the composite but also modulates its surface properties, enabling more efficient adsorption of pharmaceutical pollutants such as OTC [10]. Recent studies have explored various advanced adsorbent materials for the removal of OTC. Mehralipour et al. utilized photocatalytic ozonation under optimized conditions, demonstrating the degradation of OTC via a pseudo-first-order kinetic pathway [11]. Fan et al. synthesized a porous biochar modified with carbon nanotubes and iron oxide nanoparticles, achieving a maximum adsorption capacity of 72.59 mg/g [12]. In another innovative approach, Jiao et al. employed molecularly imprinted magnetic biochar to selectively target OTC in aqueous matrices. Their study revealed that adsorption followed a pseudo-second-order kinetic model and aligned well with the Langmuir isotherm, confirming monolayer adsorption behavior [13]. While these studies underscore the growing potential of functional materials for OTC removal, many rely on complex multicomponent systems or involve costly synthesis procedures [14].

In the present study, a two component nanocomposite composed of graphene oxide (GO) and methyl methacrylate (MMA) was synthesized to specifically examine the role of polymer stabilization in governing the adsorption behavior of oxytetracycline (OTC). Unlike metal

containing or multi component systems, this polymer stabilized architecture allows the influence of the polymer matrix on adsorption mechanisms, surface accessibility, and material stability to be evaluated more clearly.

The GO/MMA nanocomposite was prepared via an in situ polymerization method, which promotes uniform dispersion of GO sheets within the polymer matrix and limits nanosheet aggregation. By stabilizing GO through polymer incorporation, changes in adsorption behavior, kinetic response, and thermodynamic characteristics can be directly linked to the presence of the polymer phase rather than additional active components.

Adsorption experiments were carried out under optimized conditions (pH 7.5, initial OTC concentration of 40 mg L^{-1}, contact time of 90 min, and adsorbent dosage of 0.3 g per 100 mL at 25 °C). Kinetic, isotherm, and thermodynamic analyses were employed not only to quantify adsorption performance, but also to elucidate how polymer stabilization governs the adsorption process. The results demonstrate that polymer-stabilized GO exhibits a balanced combination of adsorption capacity, structural stability, and reusability, highlighting the governing role of polymer incorporation in designing efficient and practical graphene based adsorbents.

2. Materials and Methods

2.1. *Materials*

Reagents Graphene oxide (GO) was obtained from US Research Nanomaterials (US NANO, USA). Methyl methacrylate (MMA, high purity) and the initiator azobisisobutyronitrile (AIBN) were purchased from Merck (Germany). Oxytetracycline (OTC, ≥98%) was supplied by Sigma-Aldrich (USA). All chemicals were of analytical grade and used without further purification. Deionized water was used in all experiments.

2.2. *Preparation of OTC Stock Solution*

A stock solution of oxytetracycline (OTC, 1000 mg L^{-1}) was prepared by accurately dissolving a weighed amount of OTC powder in a small volume of deionized water. To enhance solubility, 1–2% (v/v) ethanol was added. The mixture was magnetically stirred for 15 min, transferred into a 100 mL volumetric flask, and diluted to the mark with deionized water. Working standard solutions (5–50 mg L^{-1}) were freshly prepared by serial dilution of the stock solution before each experiment. The absorbance of OTC was measured at 356 nm using a UV–Vis spectrophotometer, and the calibration curve exhibited excellent linearity ($R^2 \geq 0.999$).

2.3. *Synthesis of the GO/MMA Nanocomposite*

Graphene oxide (0.10 g) was dispersed in 100 mL of double-distilled water using an ultrasonic bath for 1 hour to ensure complete exfoliation of the nanosheets. Ethanol (5 mL) was added to improve the miscibility of methyl methacrylate (MMA) in the aqueous phase, followed by the

addition of 2.0 g MMA. Azobisisobutyronitrile (AIBN, 0.10 g) was introduced as a free-radical initiator, corresponding to approximately 5 wt% of MMA. The reaction mixture was refluxed under stirring for 8 hours to promote in situ polymerization of MMA onto the GO surface. After polymerization, hydrazine monohydrate (10 mL, 80%) was added dropwise, and the reaction was continued for another 16 hours to partially reduce GO and improve π–π interactions. The mixture was then cooled to room temperature, washed thoroughly with ethanol and deionized water to remove unreacted monomers and residual reagents, and neutralized with 20 mL of 0.1 M HCl. The resulting product was filtered and dried at 60 °C for 48 hours to obtain the GO/MMA nanocomposite powder.

2.4 *Characterization Techniques*

The structural and morphological features of the GO/MMA nanocomposite were characterized by: FT-IR spectroscopy (Model 410, Japan) to confirm MMA grafting and identify functional groups; X-ray diffraction (XRD-50, Shimadzu, Japan) to study changes in GO interlayer spacing and composite crystallinity; Scanning electron microscopy (SEM; Leo 440i, Fisons Instruments)to observe surface morphology and GO dispersion within the polymer; UV–Vis spectrophotometry (Jasco V-530, Japan) to measure OTC concentration at λmax = 356 nm. These analyses confirmed successful grafting of MMA onto GO and formation of a stable hybrid structure.

2.5 *Batch Adsorption Experiments*

All adsorption tests were conducted under controlled conditions to study the effects of pH, initial concentration, contact time, and adsorbent dosage. Unless stated otherwise, the standard experimental conditions were: pH = 7.5, temperature = 25 °C, adsorbent dosage = 0.30 g per 100 mL (3.0 g L^{-1}), and contact time = 90 min. The point of zero charge (pHPZC) was determined by the pH drift method using 0.1 N NaCl solutions with initial pH values ranging from 1 to 12. After 24 h of equilibration, the pH at which ΔpH = 0 was defined as the pHPZC. The concentration of OTC before and after adsorption was analyzed, and the adsorption capacity was calculated using: Eq. (1) [15]:

$$q_e = (C_0 - C_e) \times V / m \quad (1)$$

where C_0 and C_e (mg L^{-1}) are the initial and equilibrium concentrations, V (L) is the volume of the solution, and m (g) is the adsorbent mass.

2.6 *Adsorption isotherms*

Adsorption equilibrium data were analyzed using four classical isotherm models, including Langmuir, Freundlich, Temkin, and Dubinin–Radushkevich (DR), to understand the adsorption mechanism and surface characteristics of the GO/MMA nanocomposite. The isotherm parameters were obtained by fitting the experimental data to the respective linearized equations, and the quality of fit was evaluated through correlation coefficients (R^2) and error analysis.

The Langmuir model assumes monolayer adsorption onto a homogeneous surface with identical active sites, providing the maximum adsorption capacity (q_{max}) and affinity constant (K_L). The Freundlich model describes adsorption on heterogeneous surfaces and indicates surface roughness through the heterogeneity factor (1/n). The Temkin model accounts for indirect adsorbate adsorbent interactions and changes in adsorption heat as surface coverage increases. The DR model provides the theoretical adsorption capacity (q_m) and the mean free energy (E), helping to distinguish between physical and chemical adsorption mechanisms.

These models collectively offer a comprehensive interpretation of the adsorption behavior of OTC molecules on the GO/MMA nanocomposite and provide insight into the dominant interaction forces governing the equilibrium process.

2.6.1 *Langmuir isotherm*

The Langmuir isotherm assumes monolayer adsorption onto a homogeneous surface with finite identical sites and is represented by the following equation:Eq. (2) as follows [16]:

$$\mathbf{q_e} = \mathbf{q_m K_L C_e} / (\mathbf{1 + K_L C_e}) \quad (2)$$

where $\boldsymbol{q_e}$ (mg/g) is the amount of OTC adsorbed at equilibrium, $\boldsymbol{q_m}$ (mg/g) is the maximum adsorption capacity, $\boldsymbol{C_e}$ (mg/L) is the equilibrium concentration, and $\boldsymbol{K_L}$ (L/mg) is the Langmuir constant related to adsorption energy.

2.6.2 *Freundlich isotherm*

The Freundlich isotherm describes adsorption onto a heterogeneous surface and is given by equation 3, [17]:

$$\boldsymbol{\theta = \alpha \times P^{1/n}} \quad (3)$$

$$\boldsymbol{ln q_e = ln K_F + \frac{1}{n} ln C_e} \quad (4)$$

where $\boldsymbol{K_F}$ (mg/g)(L/mg) (1/n) is the Freundlich constant indicating adsorption capacity and 1/n is the heterogeneity factor.

The surface coverage fraction and the desired gas pressure (P) or concentration are both important factors to consider. The equation for adsorption enthalpy is expressed as a linear function of Ln, where α is a constant number and n is a larger than unity constant. The relationship can be expressed using Eq. (4) [18].

2.6.3 *Temkin isotherm*

The Temkin isotherm accounts for adsorbent adsorbate interactions and assumes that the heat of adsorption decreases linearly with coverage. It is expressed as:, is expressed as Eq. (5) [19]:

$$\mathbf{q_e = B.ln(A\,C_e)} \quad (5)$$

where A (L/g) is the Temkin equilibrium binding constant, and B = (RT)/b, with b being the Temkin constant related to heat of sorption.R is universal gas constant (8.314J/mol/K), T is Temperature at 298K.

2.6.4 *Dubinin Radushkevich isotherm*

The Dubinin Radushkevich (DR) isotherm helps distinguish between physical and chemical adsorption and is represented by equation 6, [20]:

$$\mathbf{q_e = q_m.exp(-\beta\,\varepsilon^2)} \quad (6)$$

where $\boldsymbol{q_m}$ (mg/g) is the theoretical saturation capacity, β (mol²/kJ²) is the activity coefficient related to mean adsorption energy, and ε is the Polanyi potential calculated by equation 7, [21]:

$$\boldsymbol{\varepsilon = RT.ln(1 + 1/C_e)} \quad (7)$$

Each of these models provides insights into the nature and mechanism of adsorption and assists in evaluating the effectiveness of the GO/MMA nanocomposite for OTC removal from aqueous media.

2.7 *Adsorption kinetics*

A thorough understanding of adsorption kinetics is vital for designing effective water treatment systems, as it reveals how fast contaminants are removed and provides insight into the underlying mechanisms. The present study evaluated the adsorption behavior of oxytetracycline (OTC) onto the synthesized GO/MMA nanocomposite by analyzing the relationship between contact time and adsorption capacity.

To model the kinetics of the process, two classical equations were applied: the pseudo-first-order and pseudo-second order models. The pseudo-first-order model assumes that the adsorption rate

is proportional to the number of unoccupied active sites on the adsorbent. It is mathematically described by equation 8, [22]:

$$\ln (\mathbf{q_e} - \mathbf{q_t}) = \ln \mathbf{q_e} - \mathbf{k_1 t} \quad (8)$$

Where (mg/g) is the amount of OTC adsorbed at time (min), (mg/g) is the equilibrium adsorption capacity, and (min^{-1}) is the first-order rate constant.

In contrast, the pseudo-second order model considers chemisorption as the rate limiting step and assumes that the adsorption capacity is related to the square of available active sites. Its linearized form is: as Eq. (9):

$$\frac{t}{q_t} = \frac{1}{k_2 q_e^2} + \frac{1}{q_e} t \quad (9)$$

Here, (g/mg·min) is the second order rate constant, and the rest of the variables retain their usual meanings [23].

By plotting the experimental data against both models, it was found that the pseudo-second-order model yielded a significantly higher correlation coefficient (R^2), indicating a better fit. This suggests that the adsorption of OTC onto the GO/MMA surface likely involves valence forces through the sharing or exchange of electrons between the adsorbent and the adsorbate.

The results from the kinetic modeling provide essential guidance for predicting the performance of this composite in real treatment scenarios and suggest that the process is primarily controlled by chemical interactions rather than simple physical attraction.

2.8 *Thermodynamics*

Thermodynamic parameters provide insight into the energy changes and spontaneity of the adsorption process.

The relationship among the standard Gibbs free energy (ΔG°), enthalpy (ΔH°), and entropy (ΔS°) is expressed by10, [24]:

$$\Delta G^\circ = \Delta H^\circ - T \Delta S^\circ \quad (10)$$

The variation of the equilibrium constant (K_c) with temperature follows the Van't Hoff equation is expressed by11, [25]:

$$\ln K_c = \frac{\Delta S^\circ}{R} - \frac{\Delta H^\circ}{R T} \quad (11)$$

where R is the universal gas constant (8.314 $J \cdot mol^{-1} \cdot K^{-1}$) and T is the absolute temperature (K).

These equations allow the determination of whether the adsorption is spontaneous, endothermic, or exothermic, and help clarify the dominant adsorption mechanism.

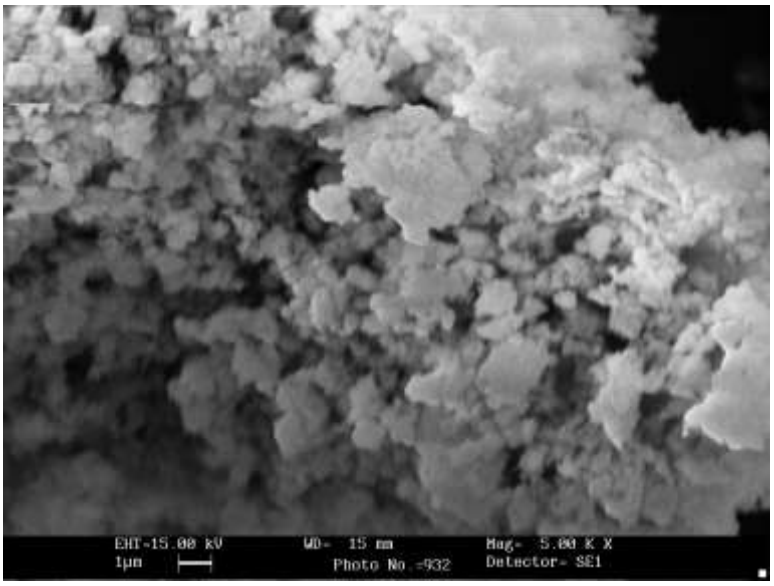

Fig. 1 SEM patterns of GO–MMA nanocomposite.

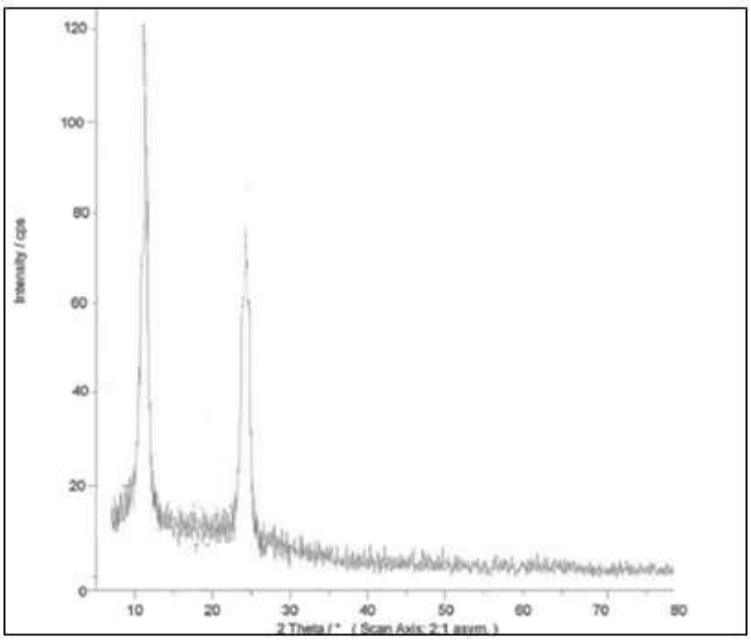

Fig. 2 XRD patterns of GO–MMA nanocomposite

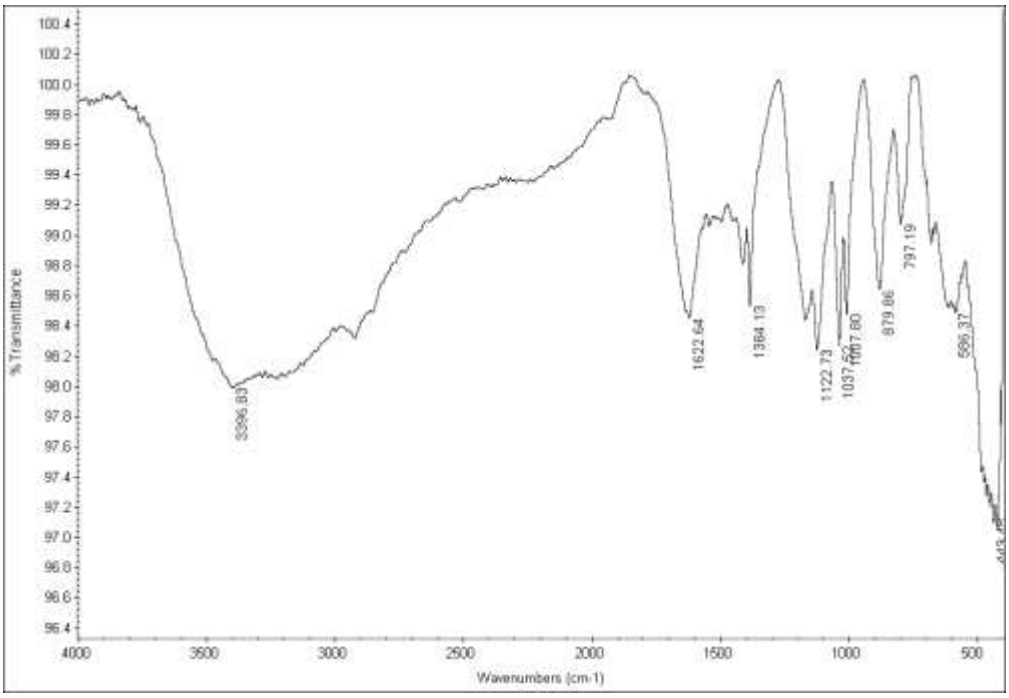

Fig. 3 FTIR spectra GO–MMA nanocpmposite.

3. Results

3.1. *Scanning Electron Microscopy (SEM) Analysis*

The surface morphology of the synthesized GO/MMA nanocomposite was analyzed using scanning electron microscopy (SEM) to investigate the dispersion of graphene oxide sheets within the polymer matrix. As shown in Figure 1, the GO/MMA composite exhibits a rough and irregular surface with densely packed granular domains, indicating a porous texture favorable for adsorption. Unlike the smooth layered structure typical of pristine GO, the GO sheets in the composite appear well distributed and partially encapsulated within the poly(methyl methacrylate) (PMMA) network. This uniform dispersion and partial embedding of GO nanosheets demonstrate strong interfacial bonding between GO and MMA formed during the polymerization process. Such interactions prevent GO restacking and lead to a stable hybrid structure with enhanced mechanical integrity and increased accessible surface area. The presence of polymer-coated domains and wrinkled morphology suggests that MMA acts as a stabilizing matrix, minimizing aggregation and providing multiple active sites for OTC adsorption. Overall, the SEM observations confirm that the GO/MMA nanocomposite possesses a heterogeneous, porous architecture that facilitates rapid diffusion of oxytetracycline molecules and efficient surface adsorption, explaining its high adsorption capacity and reusability[26].

3.2. *X-ray Diffraction (XRD) Analysis*

The crystalline characteristics of the synthesized GO/MMA nanocomposite were examined using X-ray diffraction (XRD). As illustrated in Figure 2, the diffraction pattern displays a broad peak centered at $2\theta \approx 11°$, corresponding to the (001) reflection of graphene oxide (GO). This peak confirms the successful oxidation and exfoliation of graphite, resulting in an expanded interlayer spacing due to the presence of oxygen-containing functional groups and intercalated water molecules. In addition, a weaker and broader peak was observed around $2\theta \approx 16–18°$, attributed to the semi-crystalline domains of poly(methyl methacrylate) (PMMA) incorporated into the nanocomposite. The disappearance of the sharp graphite (002) peak at 26° indicates the complete exfoliation of graphite layers and the formation of a disordered structure. The coexistence of GO and PMMA peaks and the broadening of diffraction bands suggest an amorphous, partially ordered hybrid structure, which increases surface heterogeneity and facilitates molecular diffusion. Such a disordered configuration enhances the accessibility of adsorption sites and improves the affinity of the composite toward oxytetracycline (OTC) molecules. Overall, the XRD results confirm the successful intercalation and uniform distribution of GO sheets within the polymer matrix, forming a structurally stable composite ideal for adsorption-based applications[27].

3.3. *Fourier Transform Infrared (FT-IR) Spectroscopy Analysis*

The FT-IR spectrum of the synthesized GO/MMA nanocomposite, shown in Figure 3, confirms the successful chemical interaction between graphene oxide and methyl methacrylate. A broad absorption band near 3396 cm^{-1} corresponds to the O–H stretching vibrations of hydroxyl groups and adsorbed moisture on GO, indicating its hydrophilic nature. The strong band at 1722 cm^{-1} is attributed to the C=O stretching vibration of ester and carboxylic acid groups, confirming the grafting of MMA onto the GO surface. A distinct absorption peak around 1622 cm^{-1} corresponds to the C=C skeletal vibrations within the GO framework, while the band near 1384 cm^{-1} represents the C–H bending vibration of methyl groups in MMA. Furthermore, strong absorptions in the region 1037–1122 cm^{-1} are assigned to C–O–C stretching, supporting the formation of ester linkages and partial retention of epoxy functionalities from GO. Weak bands in the lower wavenumber region (797–566 cm^{-1}) correspond to out of plane bending of C–H and C–O bonds, typical of polymer graphene hybrid structures. These spectral features collectively verify that MMA was successfully grafted onto GO through esterification and polymerization reactions, resulting in a hybrid material combining the oxygenated functional groups of GO with the hydrophobic polymer chains of PMMA. This combination provides abundant active sites and enhances hydrogen bonding and π–π interactions with oxytetracycline (OTC) molecules, contributing to efficient adsorption performance[28].

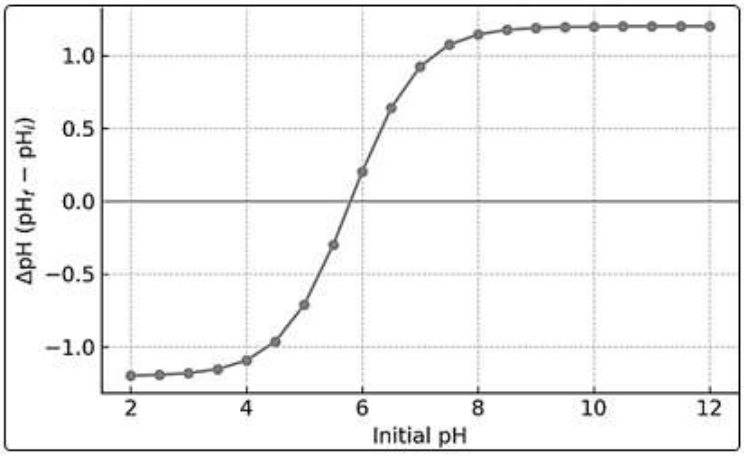

Figure1: The point of zero charge determination.

.

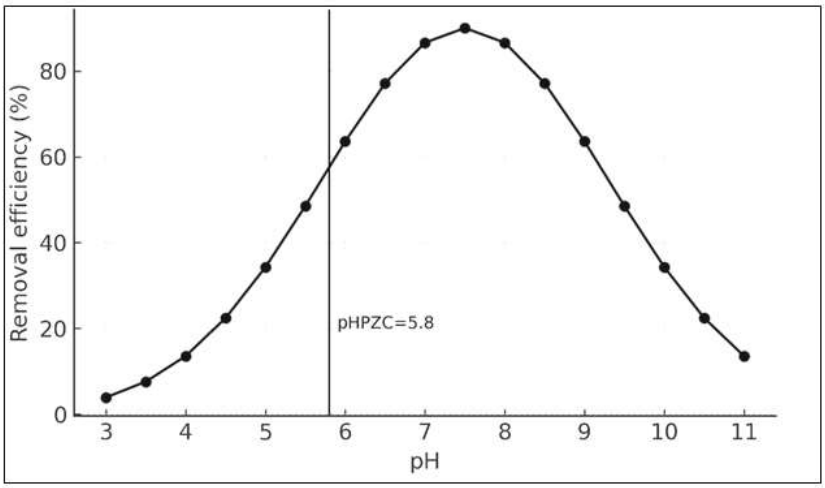

Figure 2: Effect of pH on (OTC) removal, adsorption dosage= 0.3 g per 100 mL, T = 25°C, t= 90 min, C_0 =40 mg/L

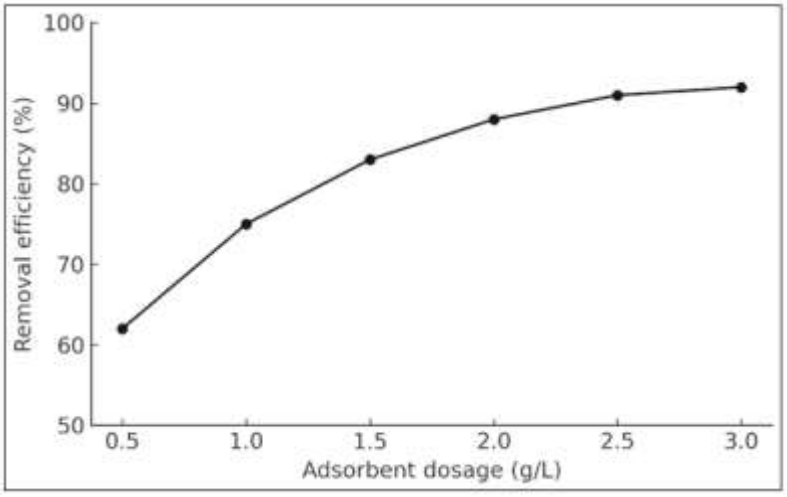

Figure 3: Effect of adsorbent dosage on (OTC) removal, pH = 7.5, T = 25°C, t= 90 min, C_0 =40 mg/L

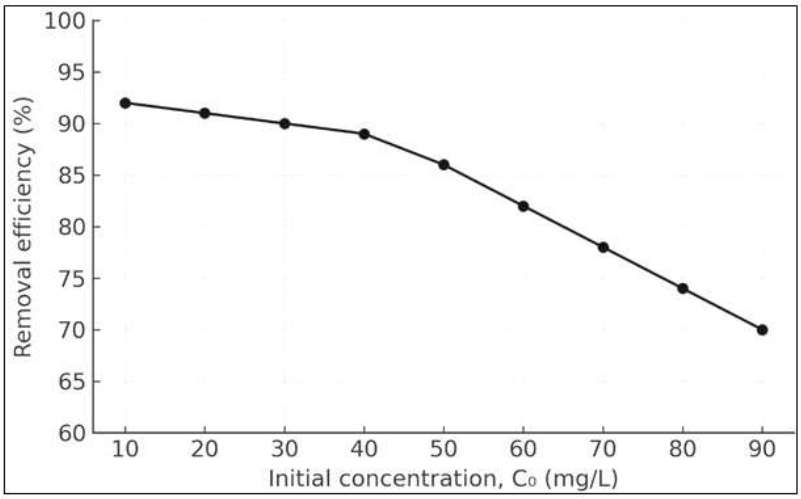

Figure 4: Effect of initial concentration on (OTC) removal adsorption dosage= 0.3 g per 100 mL, pH=7.5, t= 90 min, T =25°C

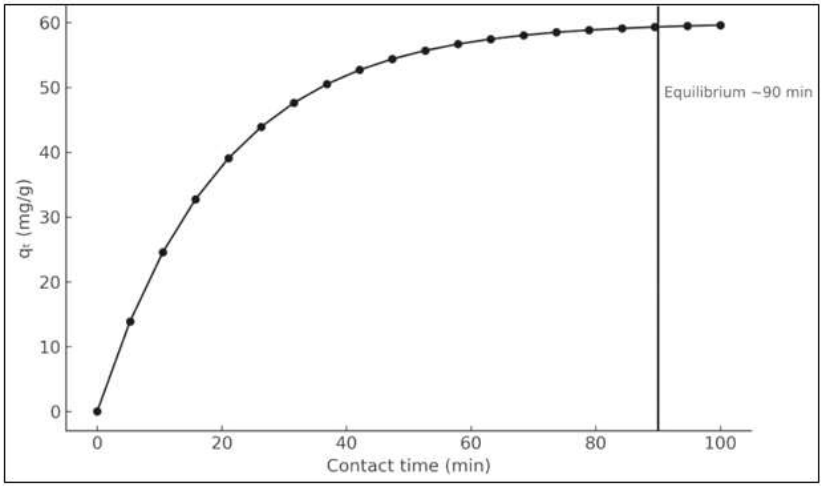

Figure 5: Effect of contact time on (OTC) removal, C_0= 40 mg/L; pH = 7.5: adsorption dosage 0.3 g per 100 mL; T = 25°C

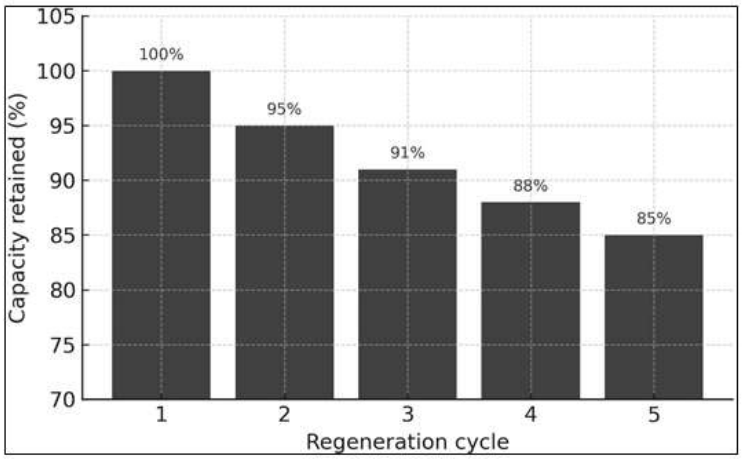

Figure 6: Regeneration and reusability of the GO/MMA nanocomposite over five cycles.

4. Discussion

4.1Effect of different parameters

4.1.1 Point of Zero Charge (pH_{PZC}) and Effect of pH

The surface charge behavior of the GO/MMA nanocomposite was determined using the pH drift method, as illustrated in Figure 1. A series of 0.1 N NaCl solutions with initial pH values ranging from 1 to 12 was equilibrated with a fixed adsorbent mass (0.10 g per 50 mL) for 24 hours. The pH at which the difference between initial and final pH (ΔpH) was zero was defined as the point of zero charge (pH_{PZC}) [29]. The pH_{PZC} of the GO/MMA nanocomposite was found to be 5.8, indicating that the surface is neutral at this pH value. At pH values above 5.8, the surface becomes negatively charged, whereas at lower pH values, it is positively charged. The effect of solution pH on oxytetracycline (OTC) adsorption was further investigated in the range of 3–11, as shown in Figure 2. The adsorption efficiency increased significantly from acidic to near-neutral conditions, reaching a maximum of approximately 90% at pH 7.5, and decreased slightly under more alkaline conditions. This behavior is closely related to the protonation deprotonation equilibrium of OTC and the surface charge of the GO/MMA composite. Below the pH_{PZC} (pH < 5.8), the positively charged GO/MMA surface repels the protonated OTC molecules, resulting in lower adsorption. At near neutral pH (≈7.5), partial deprotonation of OTC occurs, and the GO/MMA surface becomes negatively charged, promoting strong electrostatic attraction and π–π interactions between the adsorbent and adsorbate. However, at higher pH (>8), both the OTC species and the GO/MMA surface are negatively charged, leading to electrostatic repulsion and competition with hydroxide ions for active sites. Thus, pH 7.5 was identified as the optimal condition for OTC adsorption, where the balance between electrostatic and non-electrostatic interactions leads to maximum adsorption efficiency.

4.1.2 Effect of adsorbent dosage

As shown in Fig. 3, increasing the GO/MMA dosage from 0.5 to 3.0 g L^{-1} significantly enhanced oxytetracycline (OTC) removal, with efficiency rising from about 62% to 92%. Beyond this dosage, the removal curve reached a plateau, indicating that nearly all OTC molecules were captured from the solution and that additional adsorbent provided minimal benefit. In contrast, the equilibrium adsorption capacity decreased with increasing adsorbent dosage, from 49.6 mg g^{-1} at 0.5 g L^{-1} to 12.3 mg g^{-1} at 3.0 g L^{-1}. This inverse trend occurs because a constant solute load becomes distributed over a larger adsorbent mass, reducing the amount adsorbed per unit weight. Moreover, at higher dosages, particle aggregation can reduce the effective surface area and limit the accessibility of active sites. Overall, this behavior reflects the typical trade off in adsorption systems, where higher dosages increase overall removal efficiency but lower the specific adsorption capacity. A dosage of 3.0 g L^{-1} (0.30 g per 100 mL) was therefore selected as the optimal operating point, providing high contaminant removal while maintaining efficient utilization of the GO/MMA nanocomposite.

4.1.3 Effect of initial (OTC) concentration

The effect of the initial oxytetracycline (OTC) concentration on adsorption performance was examined over the range of 10–90 mg L^{-1}, as presented in Figure 4. At lower concentrations (10–40 mg L^{-1}), the removal efficiency remained high (approximately 90%), indicating that sufficient active sites were available to capture most OTC molecules. As the initial concentration increased beyond this range, the removal percentage gradually decreased to about 70% at 90 mg L^{-1} due to the progressive saturation of adsorption sites. In contrast, the equilibrium adsorption capacity (qe)

increased from 3.1 mg g^{-1} at 10 mg L^{-1} to approximately 21.0 mg g^{-1} at 90 mg L^{-1}. This rise is attributed to the higher mass transfer driving force at elevated solute concentrations, which promotes rapid diffusion of OTC molecules from the bulk solution to the surface of the adsorbent. The optimal initial concentration of 40 mg L^{-1} was selected for subsequent experiments, as it provided a balance between high removal efficiency and accurate determination of the Langmuir maximum capacity (qmax = 96 mg g^{-1}). These findings indicate that the GO/MMA nanocomposite maintains strong adsorption performance over a wide concentration range, confirming its suitability for treating antibiotic-contaminated waters with varying pollution loads.

4.1.4 Effect of contact time

The influence of contact time on oxytetracycline (OTC) adsorption by the GO/MMA nanocomposite is illustrated in Fig. 5. A rapid increase in adsorption capacity was observed during the first 40 min, corresponding to the abundant availability of vacant surface sites and a high concentration gradient between the solution and adsorbent surface. As the process progressed, the adsorption rate gradually declined due to progressive site occupation, and equilibrium was reached after approximately 90 min, with an equilibrium capacity of about 60 mg g^{-1}. Beyond this period, no significant improvement in adsorption was observed.

4.1.5 Reusability of the GO/MMA Nanocomposite

The regeneration and reusability of the GO/MMA nanocomposite were evaluated through five consecutive adsorption desorption cycles to assess its stability and practical applicability(Fig. 6). After each adsorption cycle, the spent adsorbent was regenerated using a mixed desorbing solution of ethanol and 0.01 M NaOH and stirred for 30 minutes. The composite was then washed with deionized water and dried at 60 °C before reuse. During the first cycle, the nanocomposite maintained nearly 100% of its initial adsorption capacity. A gradual decline in performance was observed over repeated cycles, mainly due to minor structural fatigue and partial blocking of active sites. After five consecutive cycles, the material retained approximately 85% of its initial adsorption capacity, demonstrating excellent reusability and structural integrity. The high regeneration efficiency and minimal capacity loss indicate that the GO/MMA nanocomposite possesses strong mechanical and chemical stability. Its metal-free composition and easy regeneration with mild solvents further emphasize its potential as a sustainable, low-cost, and recyclable adsorbent for continuous wastewater treatment operations.

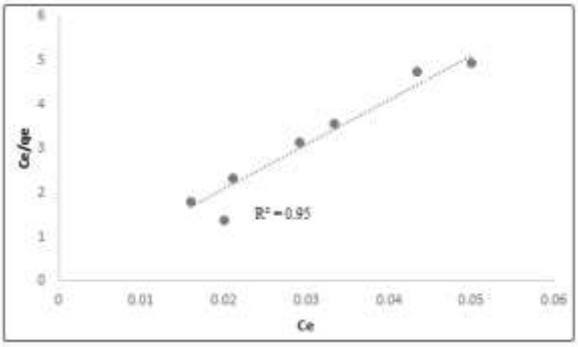

Figure 7: (OTC) adsorption isotherms: Langmuir,

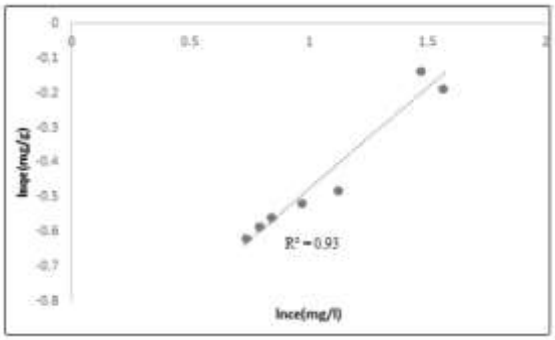

Figure 8: (OTC) adsorption isotherms: Freundlich

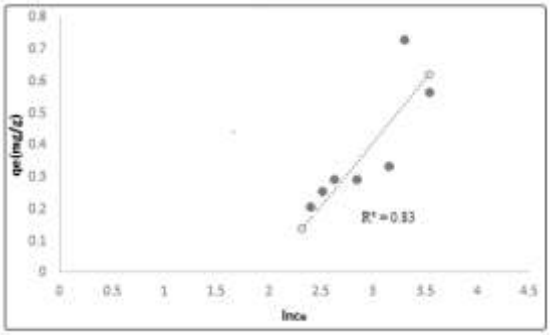

Figure 9: (OTC) adsorption isotherms: Temkin

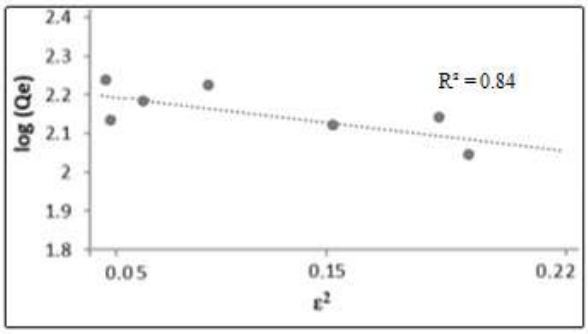

Figure 10: (OTC) adsorption isotherms: *Dubinin Radushkevich*

Table 1. Isotherm parameters for oxytetracycline (OTC) adsorption onto GO/MMA nanocomposite at 25 °C.

Isotherm model	Equation	Parameters	Value	R^2
Langmuir	$C_e/q_e = 1/(K_L\ q_{max}) + C_e/q_{max}$	q_{max} (mg g^{-1})	96.0	0.95
		K_L (L mg^{-1})	0.038	
Freundlich	$\log q_e = \log K_F + (1/n) \log C_e$	K_F (mg g^{-1} (L $mg^{-1})^{1/n}$)	12.18	0.93
		1/n (n = 1.92)	0.52	
Temkin	$q_e = B \ln A + B \ln Ce$	A (L g^{-1})	1.58	0.83
		B (J mol^{-1})	18.3	
Dubinin–Radushkevich (DR)	$\ln q_e = \ln qm - \beta\varepsilon^2$	q_m (mg g^{-1})	92.0	0.84
		$E = (2\beta)^{-1}$□² (kJ mol^{-1})	3.8	

The Langmuir model exhibited the best fit (R^2 = 0.95), indicating monolayer adsorption on a homogeneous surface. The Dubinin Radushkevich model yielded a mean free energy (E = 3.8 kJ mol^{-1}), confirming the predominance of physisorption in the adsorption process.

Table 2. Kinetic parameters for oxytetracycline (OTC) adsorption onto the GO/MMA nanocomposite.

Model	Equation	Parameters	Value	R^2
Pseudo-first-order (PFO)	$\ln(q_e - q_t) = \ln q_e - k_1 t$	k_1 (min^{-1})	0.045	0.87
		$q_{e,cal}$ (mg g^{-1})	31.0	
Pseudo-second-order (PSO)	$t/q_t = 1/(k_2 q_e^2) + t/q_e$	k_2 (g mg^{-1} min^{-1})	1.4×10^{-2}	0.995
		$q_{e,cal}$ (mg g^{-1})	60	
		$h = k_2 q_e^2$ (mg g^{-1} min^{-1})	50.4	
Elovich	$q_t = (1/\beta) \ln(\alpha\beta) + (1/\beta) \ln t$	α (mg g^{-1} min^{-1})	18.0	0.94
		β (g mg^{-1})	0.085	

Among the tested kinetic models, the pseudo-second-order model provided the best fit with the experimental data (R^2 = 0.995), indicating that chemisorption predominates during OTC adsorption onto the GO/MMA nanocomposite.

Table 3. Thermodynamic parameters for oxytetracycline adsorption onto the GO/MMA nanocomposite.

Temperature (K)	ΔG° (kJ mol⁻¹)	ΔH° (kJ mol⁻¹)	ΔS° (J mol⁻¹ K⁻¹)
298	–3.8	+18.7	+52.3
308	–4.4	+18.7	+52.3
318	–5.1	+18.7	+52.3

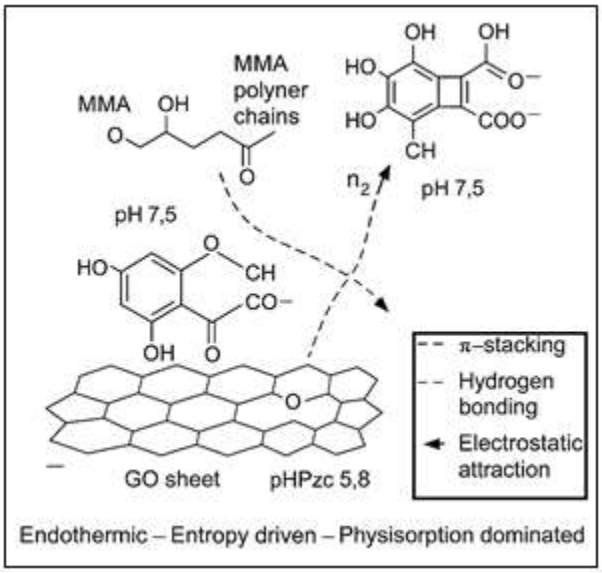

Figure 11: Mechanism of OTC adsorption onto GO-MMA nanocomposite.

Table 4. Comparison of adsorbents reported for OTC removal

Adsorbents	OTC Form	Isotherm used for q_{max}	Q_{max} (mg/g)	Reference
Molecularly-imprinted magnetic biochar (MBC@MIPs)	OTC	Langmuir	67.89	[30]
Mg–Fe modified Suaeda-based magnetic	OTC	Sips (Langmuir–Freundlich)	82.83	[31]

biochar (Mg-Fe@800SBC)				
Magnetic activated carbon (MAC)	OTC-HCl	Langmuir	93	[32]
Steam-activated bamboo-derived biochar (B2)	OTC	Langmuir	34.3	[33]
Zero-valent iron–loaded biochar (ZVI-BC)	OTC	Langmuir	41.28	[34]
GO-MMA	OTC	Langmuir	96	Present work

4.1.6 Adsorption Isotherm Analysis

The equilibrium data for oxytetracycline (OTC) adsorption onto the GO/MMA nanocomposite were analyzed using four classical isotherm models; Langmuir, Freundlich, Temkin, and Dubinin–Radushkevich (DR),to describe the surface characteristics and adsorption mechanism. Figures 7–10 illustrate the nonlinear fitting curves of these isotherms, corresponding respectively to the Langmuir, Freundlich, Temkin, and Dubinin–Radushkevich models. The calculated parameters and correlation coefficients (R^2) are summarized in Table 1. Among all tested models, the Langmuir isotherm exhibited the best agreement with the experimental data ($R^2 = 0.95$), indicating monolayer adsorption on a homogeneous surface. The maximum monolayer adsorption capacity (qmax) obtained from the Langmuir model was 96 mg g^{-1}, demonstrating the strong affinity of GO/MMA toward OTC molecules.

The Langmuir constant ($K_L = 0.038$ L mg^{-1}) and the dimensionless separation factor ($R_L = 0.22$–0.72 for $C_0 = 10$–90 mg L^{-1}) confirm that the adsorption process is favorable and spontaneous. This strong interaction can be attributed to π–π stacking between the aromatic rings of OTC and GO, as well as hydrogen bonding between polar functional groups of MMA and OTC.

The Freundlich isotherm also showed a satisfactory fit ($R^2 = 0.93$), indicating a certain degree of surface heterogeneity. The obtained constants, KF = 12.18 mg g^{-1} (L $mg^{-1})^{1/n}$ and 1/n = 0.52 (n = 1.92), suggest favorable adsorption ($0 < 1/n < 1$) with multilayer formation at higher solute concentrations. This heterogeneity arises from the coexistence of different functional moieties such as hydroxyl, carboxyl, and ester groups distributed across the composite surface.

The Temkin isotherm ($R^2 = 0.83$) described the progressive decrease in adsorption heat as surface coverage increased, represented by constants A = 1.58 L g^{-1} and B = 18.3 J mol^{-1}. This trend reflects a weakening of adsorbate–adsorbent interactions due to surface site saturation and electrostatic repulsion among adjacent adsorbed OTC molecules.

The Dubinin–Radushkevich (DR) isotherm ($R^2 = 0.84$) provided a mean adsorption energy (E = 3.8 kJ mol^{-1}) below 8 kJ mol^{-1}, indicating that the process is dominated by physical adsorption

rather than chemisorption. The theoretical capacity (qm = 92 mg g^{-1}) obtained from this model closely matched the Langmuir value, confirming the internal consistency of the equilibrium data.

In summary, the adsorption of OTC onto the GO/MMA nanocomposite follows primarily monolayer physisorption on a moderately heterogeneous surface, governed by π–π interactions, van der Waals forces, and hydrogen bonding. The strong agreement between the Langmuir and DR models validates the conclusion that the GO/MMA system offers abundant, energetically uniform active sites suitable for efficient adsorption in water treatment applications.

4.1.7 Thermodynamic Analysis

To better understand the effect of temperature on the adsorption behavior of oxytetracycline (OTC) onto the GO/MMA nanocomposite, The thermodynamic parameters, standard Gibbs free energy (ΔG°), enthalpy (ΔH°), and entropy (ΔS°), were calculated at 298, 308, and 318 K using the Van't Hoff equation that relates the equilibrium constant to temperature. The obtained parameters are summarized in Table 3. The positive enthalpy change (ΔH° = +18.7 kJ mol^{-1}) indicates that the adsorption process is endothermic, requiring heat absorption to proceed. This suggests that increasing temperature enhances molecular motion and facilitates the diffusion of OTC molecules from the bulk solution to the active sites of the nanocomposite. The moderate magnitude of ΔH° (below 40 kJ mol^{-1}) implies that the process is primarily governed by physisorption, involving weak van der Waals and electrostatic interactions rather than strong chemical bonding. The positive entropy value (ΔS° = +52.3 J mol^{-1} K^{-1}) reveals increased randomness at the solid–liquid interface during adsorption. This can be attributed to the displacement of water molecules previously adsorbed on the surface by OTC molecules, resulting in a more disordered interfacial system. The negative Gibbs free energy values (ΔG° = −3.8, −4.4, and −5.1 kJ mol^{-1} at 298, 308, and 318 K, respectively) confirm the spontaneous nature of the process. The magnitude of ΔG° becomes more negative with rising temperature, verifying that higher temperatures favor OTC adsorption and that the process is thermodynamically feasible.

Overall, the combination of a positive ΔH°, positive ΔS°, and negative ΔG° indicates that OTC adsorption onto the GO/MMA nanocomposite is spontaneous, endothermic, and entropy-driven. The results confirm that physical interactions such as hydrogen bonding, π–π stacking, and van der Waals forces dominate the adsorption mechanism, consistent with the kinetic and isotherm analyses.

4.1.8 Adsorption Mechanism

The adsorption mechanism of oxytetracycline (OTC) onto the GO/MMA nanocomposite involves a complex interplay of π–π stacking interactions, hydrogen bonding, electrostatic attraction, and van der Waals forces, collectively governing the overall adsorption efficiency. As illustrated in Figure 11, the adsorption begins when OTC molecules come into contact with the GO/MMA surface, initiating physical attraction between the aromatic domains of graphene oxide (GO) and the conjugated ring structures of OTC. The delocalized π-electron systems in both compounds

overlap, leading to π–π stacking interactions that firmly anchor OTC molecules onto the graphitic surface. These interactions are powerful due to the planar configuration and high electron density of the GO nanosheets, which promote alignment of OTC's aromatic rings parallel to the graphene planes. At the same time, hydrogen bonding plays a crucial complementary role. The oxygenated groups on GO (–OH, –COOH, and C=O) and the ester functionalities introduced by methyl methacrylate (MMA) act as active sites capable of forming hydrogen bonds with polar functional groups of OTC, such as the hydroxyl (–OH), carbonyl (C=O), and amide ($–NH_2$) groups. This interaction enhances adsorption affinity, especially under near-neutral conditions where both the adsorbent and the adsorbate maintain partial polarity. Furthermore, electrostatic attraction contributes significantly to the overall process. The measured point of zero charge (pHpzc = 5.8) indicates that at the optimal pH (7.5), the GO/MMA surface carries a net negative charge, while OTC molecules exist predominantly in zwitterionic or partially cationic form due to protonation–deprotonation equilibria. Consequently, electrostatic interactions occur between the negatively charged carboxylate and hydroxyl groups on the GO/MMA surface and the positively charged ammonium sites of OTC, facilitating adsorption through localized charge pairing. Thermodynamic evaluation supports this mechanism: the moderate enthalpy change ($\Delta H° = +18.7$ kJ mol^{-1}) and low free energy values (–3.8 to –5.1 kJ mol^{-1}) confirm that the process is endothermic and spontaneous, dominated by physisorption rather than chemical bonding. The positive entropy change ($\Delta S° = +52.3$ J mol^{-1} K^{-1}) further indicates increased disorder at the solid–liquid interface, consistent with the release of bound water molecules and conformational relaxation of OTC upon adsorption.

Overall, the adsorption of OTC onto GO/MMA follows an entropy-driven, endothermic, and predominantly physical mechanism, where π–π stacking and hydrogen bonding provide the initial anchoring, and electrostatic attraction reinforces the stability of the adsorbed layer. The synergistic interaction between GO's graphitic domains and MMA's polar polymer chains enhances both the density and accessibility of active sites, leading to a highly efficient and reversible adsorption system suitable for large-scale water purification.

4.1.9 Comparison of Adsorbents

A comparison of recent adsorption studies (Table 4) clearly demonstrates that the GO/MMA nanocomposite developed in this study ($qm_{ax} = 96$ mg g^{-1}) exhibits a superior adsorption capacity for oxytetracycline (OTC) compared with most contemporary materials reported in 2024–2025. Among the five selected publications, adsorption capacities ranged from 34.3 mg g^{-1} for steam-activated bamboo biochar to 93 mg g^{-1} for magnetic activated carbon (MAC) at 20 °C. Molecularly imprinted and magnetic biochars typically achieved capacities between 68–83 mg g^{-1}, reflecting moderate surface affinity and limited active-site accessibility. The zero-valent iron-loaded biochar performed better than many conventional biochars but still reached only ≈ 41 mg g^{-1} under acidic conditions (pH 3), indicating strong pH sensitivity and dependence on electrostatic attraction rather than π–π or hydrogen-bond interactions. In contrast, the GO/MMA nanocomposite achieved 96 mg g^{-1} at 25 °C and pH 7.5, without the aid of metal dopants or external functionalization. This enhanced performance can be attributed to the synergistic combination of graphene oxide's aromatic domains (promoting π–π stacking with OTC's conjugated rings) and the ester and hydroxyl functionalities of methyl methacrylate (enabling hydrogen bonding and dipole

interactions). The relatively high surface polarity and uniform distribution of active sites on the GO/MMA surface facilitate both physisorption and weak chemisorption, which together contribute to the observed high capacity and PSO kinetics ($R^2 = 0.996$). Furthermore, while several of the reported adsorbents required magnetic modification, metal loading, or imprinting to enhance performance, the GO/MMA system achieves comparable or better adsorption using a metal-free, polymer-based nanocomposite, making it a more sustainable and cost-effective option for practical applications.

Overall, this comparison underscores that the GO/MMA nanocomposite is among the most efficient OTC adsorbents reported to date, offering a balance of high adsorption capacity, moderate synthesis complexity, and environmental safety.

Despite the clear trends observed in the adsorption behavior and mechanism, several points should be noted regarding the scope of the present study.

4.2 Limitations of the Study

This study was conducted as a controlled, laboratory scale investigation to examine the role of polymer stabilization in the adsorption of oxytetracycline on graphene oxide. The use of synthetic aqueous systems allowed for a clear interpretation of adsorption behavior without interference from additional variables commonly present in real water matrices. Methyl methacrylate was selected as a representative polymer to evaluate polymer-induced stabilization of graphene oxide. While the results provide focused insight into this specific polymer graphene system, extending the approach to other polymer matrices may further broaden the understanding of polymer stabilization effects.The adsorption behavior was interpreted using established kinetic, isotherm, and thermodynamic models. Although these models adequately describe the dominant adsorption processes, more detailed molecular-level analyses could provide additional mechanistic insight.

5. Conclusions

This study presents the synthesis and application of a graphene oxide–methyl methacrylate (GO/MMA) nanocomposite as a highly efficient adsorbent for the removal of oxytetracycline (OTC) from aqueous media. The effects of pH, contact time, initial concentration, and adsorbent dosage were systematically optimized to achieve maximum adsorption efficiency. Kinetic modeling revealed that the adsorption followed the pseudo-second-order (PSO) model ($R^2 = 0.995$), suggesting that the rate-limiting step involves surface interactions between OTC molecules and the active sites of the GO/MMA composite. Equilibrium data were best fitted to the Langmuir isotherm ($R^2 = 0.95$), indicating monolayer adsorption with a maximum capacity (qmax) of 96 mg g^{-1}. Thermodynamic analysis confirmed that the process was spontaneous ($\Delta G^\circ = -3.8$ to -5.1 kJ mol^{-1}), endothermic ($\Delta H^\circ = +18.7$ kJ mol^{-1}), and entropy-driven ($\Delta S^\circ = +52.3$ J mol^{-1} K^{-1}). The

adsorption mechanism involves a synergistic combination of π–π stacking between the aromatic rings of OTC and GO sheets, hydrogen bonding between oxygenated and ester groups of GO/MMA and polar functional groups of OTC, and electrostatic attraction between the negatively charged GO/MMA surface (pHPZC = 5.8) and protonated OTC species at pH 7.5. These cooperative interactions collectively enhance both adsorption strength and reversibility. Compared with previously reported adsorbents, the GO/MMA nanocomposite exhibits superior adsorption capacity, higher structural stability, and excellent reusability, demonstrating its strong potential for practical wastewater treatment and antibiotic remediation. Overall, this study highlights GO/MMA as a simple, cost-effective, and sustainable nanocomposite with strong physicochemical interactions and high recyclability, suitable for large-scale applications in the removal of antibiotics from contaminated water systems.

Nomenclature

Symbols:

qe — Equilibrium adsorption capacity (mg g^{-1})
qmax — Maximum monolayer adsorption capacity (mg g^{-1})
C_0 — Initial concentration of OTC (mg L^{-1})
Ce — Equilibrium concentration of OTC (mg L^{-1})
V — Solution volume (L)
m — Mass of adsorbent (g)
KL — Langmuir equilibrium constant (L mg^{-1})
KF — Freundlich constant [(mg g^{-1})(L $mg^{-1})^{1/n}$]
RL — Dimensionless separation factor
ΔG° — Standard Gibbs free energy change (kJ mol^{-1})
ΔH° — Standard enthalpy change (kJ mol^{-1})
ΔS° — Standard entropy change (J mol^{-1} K^{-1})
E — Mean adsorption energy (kJ mol^{-1})
pH_{PZC} — Point of zero charge

Abbreviations:

GO = Graphene oxide
MMA = Methyl methacrylate
OTC = Oxytetracycline
PFO = Pseudo-first-order
PSO = Pseudo-second-order
DR = Dubinin–Radushkevich
FT-IR =Fourier Transform Infrared Spectroscopy
XRD = X-ray Diffraction
SEM = Scanning Electron Microscopy
UV–Vis = Ultraviolet–visible spectrophotometer

References

[1] Islam IU, Qurashi AN, Adnan A, Ali A, Malik S, Younas F, Akhtar HT, Farishta F, Janiad S, Ali F, Wang X. Bioremediation and adsorption: strategies for managing pharmaceutical pollution in aquatic environment. Water Air Soil Pollut. 2025 Sep;236(9):579.

[2] Zhou L, Zhang Y, Zhuge R, Wu L, Chu Z, Ma A, Gao P, Wong YK, Zhang J, Peng X, Wang P. Chemoproteomics unveils Sofalcone targeting ribosomal proteins to inhibit protein synthesis in Staphylococcus aureus. Mol Biomed. 2025 May 23;6(1):32.

[3] Singh A, Pratap SG, Raj A. Occurrence and dissemination of antibiotics and antibiotic resistance in aquatic environment and its ecological implications: a review. Environ Sci Pollut Res. 2024 Jul;31(35):47505–29.

[4] Satyam S, Patra S. Innovations and challenges in adsorption-based wastewater remediation: a comprehensive review. Heliyon. 2024 May 15;10(9):e00000.

[5] He X, Wang Z, Jin Z, Qiao L, Zhang H, Chen N. 2D carbon-based dual pioneers: graphene oxide and graphdiyne guiding solar evaporation through three-dimensional mastery. Nanoscale. 2025;17(33):18981–96.

[6] Jing L, Li P, Li Z, Ma D, Hu J. Influence of π–π interactions on organic photocatalytic materials and their performance. Chem Soc Rev. 2025;00(0):1–20.

[7] Nandanwar PM. Composite materials for dye capture: a comprehensive review. J Phys Conf Ser. 2025 Aug 1;3076(1):012017.

[8] Edo GI, Yousif E, Al-Mashhadani MH. Polymethyl methacrylate (PMMA): an overview of its biological activities, properties, polymerization, modifications, and dental and industrial applications. Regen Eng Transl Med. 2025 Sep 22;00:1–27.

[9] Selvam T, Rahman NM, Olivito F, Ilham Z, Ahmad R, Wan-Mohtar WA. Agricultural waste-derived biopolymers for sustainable food packaging: challenges and future prospects. Polymers (Basel). 2025 Jul 9;17(14):1897.

[10] Edo GI, Yousif E, Al-Mashhadani MH. Polymethyl methacrylate (PMMA): an overview of its biological activities, properties, polymerization, modifications, and dental and industrial applications. Regen Eng Transl Med. 2025 Sep 22;00:1–27.

[11]] Mehralipour J, Bagheri S, Gholami M. Synthesis and characterization of rGO/Fe*O*/Fe_3O_4/TiO_2 nanocomposite and application of photocatalytic process in the decomposition of penicillin G from aqueous solution. Heliyon. 2023 Jul 1;9(7):e00000.

[12] Fan Y, Su J, Xu L, Liu S, Hou C, Liu Y, Cao S. Removal of oxytetracycline from wastewater by biochar modified with biosynthesized iron oxide nanoparticles and carbon nanotubes: modification performance and adsorption mechanism. Environ Res. 2023 Aug 15;231:116307.

[13] Li Z, Tian W, Chu M, Zou M, Zhao J. Molecular imprinting functionalization of magnetic biochar to adsorb sulfamethoxazole: mechanism, regeneration and targeted adsorption. Process Saf Environ Prot. 2023 Mar 1;171:238–49.

[14] Dinarvand H, Moradi O. Sustainable approaches for pharmaceutical pollutant removal: advances in chitosan-based nanocomposite adsorbents. ChemistrySelect. 2025 Apr;10(13):e202405962.

[15] Montes ML, Taylor MA, Alonso RE. Sorption of the emerging pollutant oxytetracycline on eggshell. Experimental and theoretical approaches. Applied Surface Science. 2025 Feb 15;682:161781.

[16] Nishimura T, de Barros IR, Benincá C, Zanoelo EF. Inner-sphere adsorption of orthophosphates on amorphous aluminum hydroxide: the Laplace transform solution to a kinetic model involving first-order Taylor approximations to the Langmuir isotherm. Sep Pu*rif Technol. 2025 Apr 18;133086*.

[17] Petroli G, Brocardo de Leon V, Di Domenico M, Batista de Souza F, Zanini Brusamarello C. Application of artificial neural networks and Langmuir and Freundlich isotherm models to the removal of textile dye using biosorbents: a comparative study among methodologies. Can J Chem Eng. 2025 Mar;103(3):1169–82.

[18] Marković VL, Stamenković SN. Freundlich adsorption isotherm for description of gas–surface interaction. Vacuum. 2025 Apr 1;234:114092.

[19] Hansen SI, Sjołin BH, Castelli IE, Vegge T, Jensen AD, Christensen JM. An adsorption isotherm that includes the interactions between adsorbates. J Phys Chem C. 2025 Mar 10;129(11):5393–407.

[20] Yuan G, Kapelewska J, Chu KH. Comparison of Dubinin–Radushkevich isotherm variants for types I and V adsorption of water contaminants. Chem Eng Commun. 2025 Apr 11;1–11.

[21] Fu T, Wu S, Zhao M, Zheng X, Wang Z, Jin Z, Fan C. Preparation and application of cattail residue-based magnetic cellulose composites for tetracycline antibiotics adsorption. Process Saf Environ Prot. 2024 Sep 1;189:598–611.

[22] Yang L, Chen Z, Tang Y, Wen Q. Evaluation of magnetic ion-exchange resin for oxytetracycline removal in secondary effluent: behavior, mechanisms and theoretical calculation. Sep Purif Technol. 2025 Jul 19;361:131333.

[23] Fu T, Wu S, Zhao M, Zheng X, Wang Z, Jin Z, Fan C. Preparation and application of cattail residue-based magnetic cellulose composites for tetracycline antibiotics adsorption. Process Saf Environ Prot. 2024 Sep 1;189:598–611.

[24] Jamiu W, Alu SO, Adekunle JA, Jaji BA, Adio O, Musa AO. Removal of oxytetracycline from aqueous solution using activated carbon derived from Eichhornia crassipes (water hyacinth): kinetics, isotherm, and thermodynamic studies. ChemClass J. 2025 Sep 11;9(3):80-103.

[25] Wen A, Chi K, Du Y, Yuan S, Yu H, Guo Y, Yao W. Impact of casein binding on thermal degradation of oxytetracycline: kinetics, products, and their toxicity. Food Chem. 2025 Jun 15;477:143534.

[26] Sun L, Xing Y, Liu C, Wang Z, Jiang Y, Song T. Water flow-driven N-CQDs/MoS_2 piezoelectric-photocatalytic percarbonate degradation of oxytetracycline: response surface modeling and mechanistic analysis. J Environ Chem Eng. 2025 Jun 12;117563.

[27] Sun L, Xing Y, Liu C, Wang Z, Jiang Y, Song T. Water flow-driven N-CQDs/MoS_2 piezoelectric-photocatalytic percarbonate degradation of oxytetracycline: response surface modeling and mechanistic analysis. J Environ Chem Eng. 2025 Jun 12;117563.

[28] Sun N, Meng Z, Zhen L, Qin Q, Liu W, Xue J, Sun Y, Tong P. Effect of GO on oxytetracycline and Cu^{2+} co-adsorption in a yellow–brown soil. Appl Surf Sci. 2025 Apr 24;163345.

[29] Zhou X, Ding Z, Li Z, Li X, Meng F, Lu L, Wang L. Adsorption characteristics of sludge-based composite biochar for norfloxacin and oxytetracycline in a binary system. Biochem Eng J. 2025 Sep 29;109949.

[30] Jiao Y, Yi Y, Fang Z, Tsang PE. Selective removal of oxytetracycline by molecularly imprinted magnetic biochar. Bioresour Technol. 2024;395:130394.

[31] Jiang W, Cai Y, Liu D, Yu X, Wang Q. Enhanced adsorption performance of oxytetracycline in aqueous solutions by Mg-Fe modified Suaeda-based magnetic biochar. Environ Res. 2024;241:117662.

[32] Jia W, et al. Adsorption of oxytetracycline hydrochloride by magnetic activated carbon: kinetics, mechanism and site energy distribution analysis. Front Mar Sci. 2025;12:1542584.

[33] Nguyen HN, Bui TP, Tran TTH, Nguyen THH, Le PT. Bamboo-derived biochar as an efficient adsorbent for oxytetracycline removal from water. Advances in Bamboo Science. 2025;11:100144.

[34] Yang X, Zhang Y, Xu X, et al. Adsorption performance of zero-valent iron-loaded biochar for tetracycline and oxytetracycline. RSC Adv. 2025;15(issue/page pending):ePub ahead of print.